Arch. Metall. Mater. **65** (2020), 1, 99-102

DOI: 10.24425/amm.2019.131101

A. BIRYUKOV[1*], R. GALIN[2], D. ZAKHARYEVICH[1], A. WASSILKOWSKA[3],
A. KOLESNIKOV[1], T. BATMANOVA[1]

A LAYER-BY-LAYER ANALYSIS OF THE CORROSION PROPERTIES OF DIFFUSION ZINC COATINGS

To obtain anti-corrosive thermo-diffusion zinc coatings, the authors use highly effective zinc saturating mixtures. This technology makes it possible to obtain coatings with a high zinc content in the δ-phase as well as a zinc-rich phase of $FeZn_{13}$ (ζ-phase) on the coating surface. As a result of long-term studies into the corrosion properties of thermo-diffusion zinc (TDZ) coatings conducted by the authors, a number of features of their corrosive behavior have been established. The corrosion rate of those coatings in desalted and chloride-containing media is lower than those of galvanic or hot-dip zinc coatings. The corrosion behavior depends on the content of zinc on the surface and the texture features of the coating. The results showed that on the surface of thermo-diffusion coatings in the corrosion on media containing chloride ions, zinc hydroxychloride (simonkolleite – $Zn_5Cl_2[OH]_8[H_2O]$) has been formed. Compared to coatings obtained by other methods, the rate of simonkolleite formation was higher on TDZ coatings, which might have a positive effect on their resistance in aggressive atmospheres.

Keywords: diffusion zinc coatings, δ-phase, texture, simonkolleite

1. Introduction

A thermal-diffusion zinc coating (TDZ) is a type of protective zinc coating deposited on steel products from the vapor phase when in contact with zinc-based powders at temperatures close to the melting point of zinc (419°C). The process, which is also called sherardizing, has an advantage over electro-deposition and hot-dip galvanizing, consisting of higher adhesion and uniformity of coatings [1,2]. They are also sometimes considered to be more resistant to corrosion than other coatings. In contrast to the other types, such coatings consist of intermetallic Fe-Zn phases without pure Zn on the surface. Depending on the process parameters (time, temperature and powder composition) the coating surface can contain Γ, δ and ζ phases. A coating of typical thickness (10-60 μm) contains predominantly δ phase with a thin layer of Γ at the coating-steel interface. Special powders for thermal diffusion galvanizing, developed by the author [3], consisting of zinc particles coated with nanostructured zinc oxide [4], significantly improve the efficiency and controllability of the process.

Recent work on the corrosion behavior of TDZ coatings in a chloride-containing solution has shown the non-monotonic dependence of corrosion current on the composition of the δ phase on the coating surface with a minimum at 90 wt.% Zn [5]. Therefore the composition, along with thickness, should be taken into account when evaluating the corrosion resistance of the coating.

A structural study of TDZ coatings has shown that the δ-phase on their surface could have various crystallographic textures [6]. Thus, for relatively thick coatings (>30 μm) the δ-phase is characterized by the absence of texture, whereas the inner layer of the coating has a texture, characterized by the hexagonal axis of the δ-phase directed parallel to the plane of the coating, which is typical for the δ-phase obtained after annealing hot-dip zinc coatings [7,8]. It is known that texture could be an important factor which influences the coating properties. The rate of corrosion is generally lower for most close-packed crystallographic planes due to the stronger binding of atoms. Another mechanism of texture influence on corrosion is the nature of protective films formed on different planes. These effects were demonstrated for electrodeposited and hot-dip zinc coatings [9-12]. Then, taking into account the results of a previous work [6], it is necessary to investigate the effect of texture, along with chemical composition, on the corrosion properties of TDZ coatings. In this paper,

[1] CHELYABINSK STATE UNIVERSITY, CHELYABINSK, RUSSIAN FEDERATION
[2] VIKA GAL 2 LTD., CHELYABINSK, RUSSIAN FEDERATION
[3] CRACOW UNIVERSITY OF TECHNOLOGY, 24 WARSZAWSKA STR., 31-155 KRAKÓW, POLAND

* Corresponding author: st4857@yandex.ru

we study the corrosion behavior of coating layers of various compositions and crystallographic texture obtained by chemical layer-by-layer dissolution of TDZ coatings.

2. Experimental

Diffusion zinc coatings were applied to samples of C45 steel in the form of circular disks of the diameter 30.0 mm and thickness 3.0 mm, with a hole for hanging. The galvanizing was carried out according to the procedure in ref. [1] at 450°C for 3 hours using a saturating powder mixture containing zinc particles with a nanostructured oxide on the surface [3]. The coating thickness was determined using a magnetic thickness gauge.

In that study, samples with a thickness of 40 μm and a surface composition represented by the δ-phase ($FeZn_{7-10}$) were used. For layer-by-layer investigation of the structural and corrosion characteristics, all coatings were chemically etched in a solution of 6 wt. % nitric acid, then washed with distilled water and mechanically purified. The etching time was chosen so as to obtain a series of samples with a decreasing coating thickness, with an average pitch of 5 μm. The thickness decrease was determined using a gravimetric method.

Phase analysis of the coating surface was performed before and after the corrosion tests with a DRON-3 X-ray diffractometer using Cu Kα-radiation (speed 1°/min, 2θ from 20° to 60°). The metallographic and chemical analyses were carried out with the scanning electron microscopy technique, using a JSM-6460 LV microscope from JEOL equipped with an energy dispersive spectrometer (EDS) from Oxford Instruments.

Corrosion studies were performed in a solution of 3 wt. % NaCl. To obtain the polarization curves, a clamp cell for flat electrodes filled with a working solution was used. A silver chloride electrode was used as a reference (the potentials were next recalculated into a standard hydrogen scale), where the graphite electrode served as an auxiliary one. Polarization curves were obtained in the potential range from –1.5 V to –0.5 V with a sweep rate of 0.02 V/s. The corrosion current was calculated using extrapolation of the anodic and cathodic curves. Polarization curves and corrosion current were obtained before exposure and after exposure for 5 and 30 days in the corrosion environment. Before the polarization curves, all samples were kept in the NaCl solution for 5-10 minutes. After 30 days of exposure, the phase composition and morphology of the corrosion products were determined.

3. Results and discussion

The X-ray diffraction patterns of the specimen surface after sequential etching of the coating are presented in Fig. 1. According to the results of the X-ray phase analysis of the coating layers obtained after etching, only the maxima of the δ-phase ($FeZn_{7-10}$) are present in all layers. However, the diffraction pattern changes with coating thickness. The XRD pattern of the original coating (without etching) shows maxima (1.4.14) and (3.0.22) with a third Miller index high. After a few sequential etchings, those maxima practically disappear, while the relative intensity of the maxima with a zero third index increases, i.e. (330) and (500). Subsequent etching of the coating reveals further increases in the relative intensity of the maxima with a zero third index, i.e. the increase in the texture of the δ-phase. Thus, on the surface of the coating, the δ-phase crystals of different orientation are present, whereas in coating layers below 15 μm, crystals with a 6th-order c-axis parallel to the coating surface prevail. The scanning electron microscopy analysis showed that the zinc content near the coating surface is rather high and reaches 92 wt. %. The iron concentration in the coating layers etched down up to 15 μm amounts to about 8 wt %, then it sharply increases with the depth of coating etching.

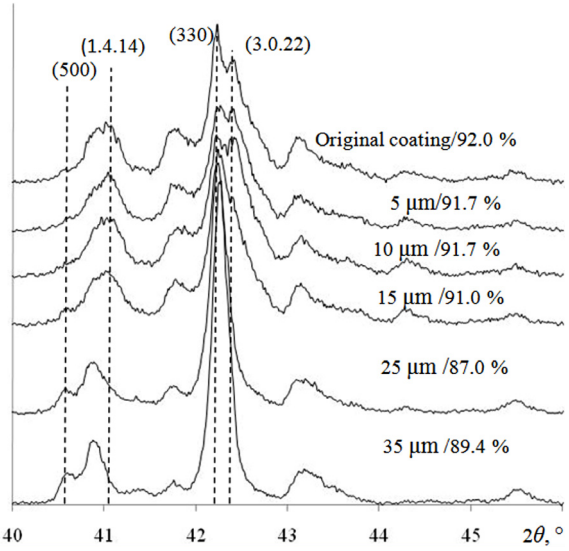

Fig. 1. X-ray diffraction patterns of coating samples with different etching depth (in mm) and the respective change in zinc content (in wt. %). The lines show the positions of the maxima of the δ-phase mentioned in the text

At the etching depth of 15 μm, there is not only a change in the elemental composition and the texture state of the δ-phase constituting the diffusion zinc coating, but the corrosion characteristics of the material under study also change. When analyzing the polarization curves of the coating layers (Fig. 2), differences in their corrosive behavior are noticeable. The cathode curves show no kinks in the potential range from –1.3 to –1.1 V and the slope of the curve decreases as it approaches the substrate. However, the quantity of electricity, corresponding to the reduction process, is smaller for coating layers from 0 to 15 μm, compared to the values measured for the layers etched deeper (20-30 μm). The decrease in the corrosion current density in this case is due to the inhibition of the depolarizer-oxygen reduction process and, accordingly, due to the smaller accumulation of the reduction products of hydroxide ions.

In the potential region from –1.0 V to –0.85 V, a decrease in current on the anode curves is observed. This is connected, apparently, with the adsorption of negatively charged ions and the formation of oxidation products on the surface of the electrode.

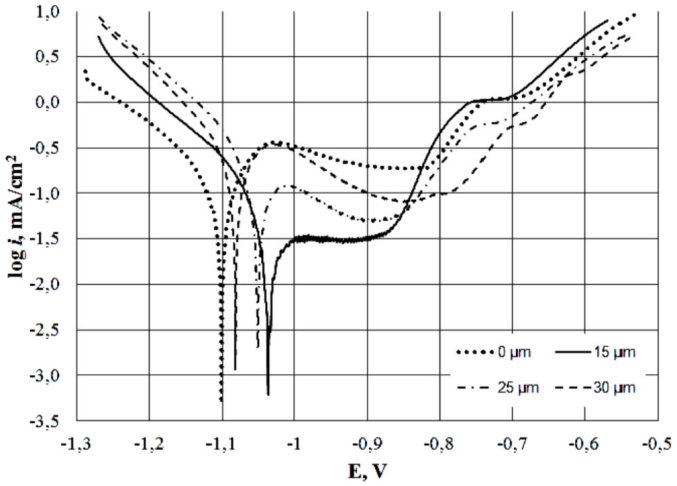

Fig. 2. Polarization curves of the coating layers

In the coating layers etched from 0 to 15 μm, the corrosion current density remains constant, whereas closer to the substrate it decreases with increasing electrochemical potential. The minimum value of the anode current corresponds to the specimen 15 μm /91 % Zn. In the potential region above –0.8 V, the current increases uniformly for all layers of the coating.

Table 1 shows the values of corrosion current [mA/cm^2] for different layers of the coating and exposure time in 3% NaCl up to 30 days, as calculated from the slopes of the cathode and anode curves. The minimum value is also observed for the 15 μm coating layer. Further strengthening of the δ-phase texture is accompanied by an increase in the corrosion current.

TABLE 1

Variation of the corrosion current with increasing exposure time of coatings: ($i_{corr}^{t}/i_{corr}^{0}$) current ratio after and before specimen holding in 3 wt. % NaCl for the time t [days]

Depth of etching, mm	i_{corr}, mA/cm^2			$i_{corr}^{5}/i_{corr}^{0}$	$i_{corr}^{30}/i_{corr}^{0}$
	0 days	5 days	30 days		
0	0.078	0.071	0.034	0.9	0.5
5	0.051	0.022	0.017	0.4	0.3
10	0.039	0.015	0.016	0.4	0.4
15	0.018	0.011	0.059	0.6	3.3
20	0.039	0.012	0.045	0.3	1.2
25	0.047	0.010	0.022	0.2	0.5
30	0.094	0.011	0.005	0.1	0.1

Table 1 also shows the corrosion current ratio ($i_{corr}^{t}/i_{corr}^{0}$) after and before specimen holding for the time t [days] in a corrosive environment. After 5 days, the corrosion current decreases in all layers of the coating ($i_{corr}^{5}/i_{corr}^{0} < 1$). However, for the exposure time of 30 days, an increase in the corrosion current compared to the initial one ($i_{corr}^{30}/i_{corr}^{0} > 1$) was detected for both the 15 μm and 20 μm layers investigated. A prolonged corrosion process of the coating layer of 15 μm (with a minimum corrosion current) results in an almost threefold increase in the corrosion rate.

Figure 3 shows the changes in the X-ray diffraction patterns of the investigated coating layers compared to the initial results of the phase-analysis presented in Figure 1, where it could be seen that, after 30 days of the corrosion process, the δ phase remained in all layers of the coating. The texture of the δ-phase on the surface of the samples after corrosion was not studied due to the strong broadening of its maxima. Nevertheless, the increase in the relative intensity of the (330) maximum observed with increases in the etching depth indicates the appearance of δ-phase texture in the deep layers of the coating, as was the case before the corrosion tests (Fig. 1). After 30 days of corrosion tests, the X-ray diffraction patterns reveal characteristic maxima from simonkolleite (zinc hydroxochloride). The analysis of the coating surface using scanning electron microscopy (Fig. 4) with a respective chemical analysis revealed the following composition (Table 2): 37.3-30.9 at. % of zinc, 55.7-60.3 at. % of oxygen, 0.9-2.3 at. % of chlorine and 0.2-1.3 at. % of iron. The

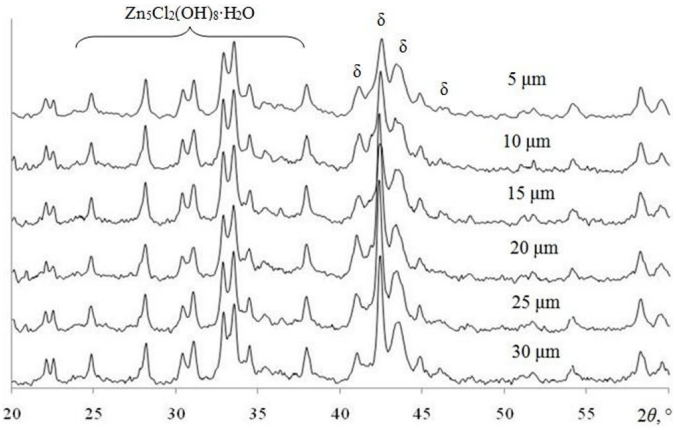

Fig. 3. X-ray patterns of samples with different etching depth after aging in NaCl solution for 30 days

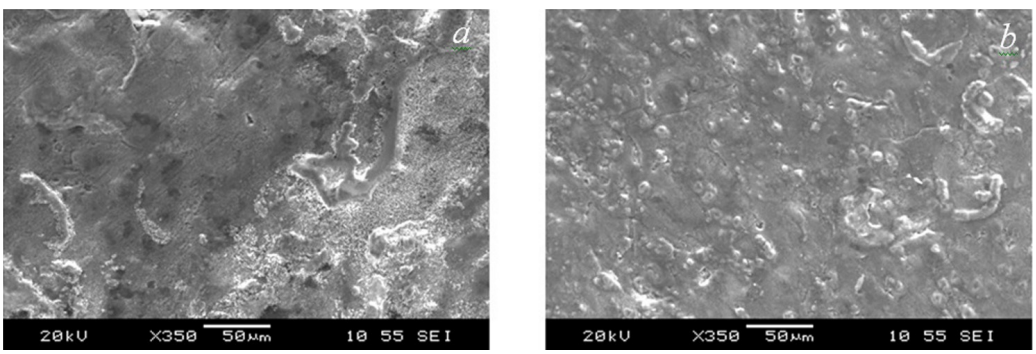

Fig. 4. SEM images of two coating samples with different etching depths: a – 15 μm; b – 30 μm after 30 days of exposure in 3 wt. % NaCl

EDS analysis was carried out at a magnification of 100×, where each area amounted to 300×200 μm. It should be noted that the maximum content of 2.3 at. % chlorine was observed in the film formed on the surface of the layer with an etching depth of 15 μm.

TABLE 2

The chemical composition of the surface of the samples after exposure for 30 days in 3 wt. % NaCl according to EDS

Depth of etching, mm	Chemical element, at. %			
	O	Cl	Fe	Zn
0	60.3	1.4	0.8	37.6
5	59.1	1.7	0.9	38.3
10	59.8	1.7	1.2	37.3
15	57.3	2.3	1.1	39.3
20	55.7	1.5	0.7	42.2
25	58.2	0.9	1.1	39.9
30	58.1	1.1	1.3	39.5

The results obtained in this work prove that major impacts on the corrosion properties of the δ-phase are exerted by both its structural features and the iron content distribution in the coating cross-section. The samples etched to 15-25 μm are characterized by a sharp change in the character of the X-ray diffraction pattern (Fig. 1). The intensity growth of the maxima with a zero third index points towards the presence of δ-phase crystal lattice faces with an excess of energy, thus influencing the corrosive behavior. Polarization measurements show minimum cathode current in the 15 μm etched layer (Table 1), which means a decrease in the intensity of the reduction reaction. As a consequence, the content of hydroxide ions on the surface of the metal becomes lower. A shift into the positive region of potential causes the absorption of chloride ions on the metal surface, which then move away the other components. The displacement by chloride ions of OH^- ions and water molecules, capable of passivating the metal surface, leads to an increase in the corrosion current at long corrosion exposures. Thus, the increase in the corrosion rate for all coating layers, except the one of 15 μm etching depth, could be associated with this phenomenon.

The iron content distribution also influences the corrosive behavior of the layers in the coating cross-section at long exposure times. The top coating layers – from the original specimen to the 15 μm etching depth – contain practically constant iron concentrations, thus the decrease in the corrosion current of those layers after 30 days of exposure was the same. The increase in the iron concentration for coating layers from 15 μm to 30 μm (Fig. 1) correlates with a decrease in the corrosion current (Table 1). Apparently, the increase in the iron concentration could have a positive effect on the formation of corrosion products enhancing the protective properties of the coating. A similar effect on the chemical stability of the compound with simonkolleite structure was reported in ref. [13] by the addition of nickel to zinc. According to the authors of [13], the nickel impurity could suppress the crystal growth of simonkolleite, so the more dense and compact layer of corrosion products inhibits the sorption of corrosive gases on the coating surface.

4. Conclusions

A great influence on the corrosion behavior of coatings consisting of the δ-phase is due to its structural properties, as well as the distribution of elements along the coating profile. The layer analysis showed that corrosion behavior varies non-uniformly with the coating thickness. If the reduction in corrosion current for layers up to 15 μm etching depth is related to the content of zinc in the δ-phase, then a further increase in the corrosion current correlates to an increase in the degree of texture in the δ-phase. The influence of corrosion products on the corrosion resistance of the layers of diffusion zinc coatings is ambiguous. The corrosion rate for each of the layers with a maximum zinc content in the δ-phase exceeds the corrosion rate for layers with a minimum zinc content by about 6 to 7 times.

REFERENCES

[1] E.V. Proskurkin, N.S. Gorbunov, Galvanizing Sherardizing and other Zinc Diffusion Coatings. Translated from Russian by D.E. Hayler. Stonehouse, Technicopy Limited, Gloucestershire, 1972.

[2] F. Natrup, W. Graf, Thermochemical Surface Engineering of Steels **62**, 737-750 (2015). DOI: 10.1533/9780857096524.5.737

[3] R.G. Galin, Patent RF No 2170643: Modified Zinc Powder, from 12. October 2000, publ. July 2001 (in Russ.).

[4] A. Wassilkowska, R. Galin, Study of zinc oxide nanopores structure on powder medium for TDG, in: Proc. of the V Int. Conf. on Electron Microscopy : EM2014, Kraków, Poland, 15-18.09.2014, AGH University of Science and Technology [et al.], Akapit, Kraków, 2014.

[5] A.I. Biryukov, R.G. Galin, D.A. Zakharyevich, A.V. Wassilkowska, T.V. Batmanova, Surface and Coatings Technology **372**, 166-172 (2019). DOI: 10.1016/j.surfcoat.2019.05.029.

[6] R.G. Galin, D.A. Zakharyevich, S.V. Rushitz, Materials Science Forum **870**, 408-412 (2016). DOI: 10.4028/www.scientific.net/MSF.870.404.

[7] V. Rangarajan, C.C. Cheng, L.L. Franks, Surface and Coatings Technology **56**, 209-214 (1993). DOI: 10.1016/0257-8972(93)90253-K

[8] A. Chakraborty, R.K. Ray, S. Sangal, Metall and Mat Trans A **39** (10), 2416-2423 (2008). DOI: 10.1007/s11661-008-9589-z

[9] H. Park, J.A. Szpunar, Corrosion Science **40** (4-5), 525-545 (1998). DOI: 10.1016/S0010-938X(97)00148-0

[10] S. Khorsand, K. Raeissi, M.A. Golozar, Corrosion Science **50** (8), 2676-2678 (2011). DOI: 10.1016/j.corsci.2011.04.007.

[11] H. Asgari, M.R. Toroghinejad, M.A. Golozar, Applied Surface Science **253** (16) 6769-6777 (2007). DOI: 10.1016/j.apsusc.2007.01.093

[12] R. Parisot. S. Forest, A. Pineau et al., Metall. Mater. Trans. A **35**A, 813-823 (2004). DOI: 10.1007/s11661-004-0008-9.

[13] H. Tanaka, N. Moriwaki, T. Ishikawa, T. Nakayama, Advanced Powder Technology, **26** (2), 612-617 (2015) DOI: 10.1016/j.apt.2015.01.010.